Origin of excitonic luminescence in quantum wells: Direct comparison of the exciton population and Coulomb correlated plasma models

J. Szczytko,* L. Kappei, J. Berney, F. Morier-Genoud, M. T. Portella-Oberli, and B. Deveaud

Institut de Photonique et Electronique Quantiques, Ecole Polytechnique Fédérale de Lausanne (EPFL), CH1015 Lausanne, Switzerland

We report on the origin of the excitonic luminescence in quantum wells. This study is carried out by time-resolved photoluminescence experiments performed on a very high quality InGaAs quantum well sample in which the photoluminescence contributions at the energy of the exciton and at the band edge can be clearly separated and traced over a broad range of times and densities. This allows us to compare the two conflicting theoretical approaches to the question of the origin of the excitonic luminescence in quantum well: the model of the exciton population and the model of the Coulomb correlated plasma. We measure the exciton formation time and we show the fast exciton formation and its dependence with carrier density. We demonstrate, by comparing the temperature dependence of $1s$ and $2s$ excitonic transitions, that excitons provide the dominant contribution to the luminescence signal. Furthermore, our analysis gives evidence that the Coulomb correlated plasma contribution to the luminescence signal might be neglected for densities, temperatures, and time scales actually used in time-resolved experiments.

I. INTRODUCTION

The work of Weisbuch *et al.*, more than 20 years ago,[1] introduced for the first time the idea that free excitons dominate the photoluminescence (PL) spectra of quantum wells at low temperatures. This appeared at the time to be in strong contrast with the observations made in bulk semiconductor samples. The reason for this major difference was later traced back to the breakdown of the translational invariance of excitons in quantum wells allowing the nonradiative polaritons in bulk semiconductors to become radiative excitons in quantum wells, quantum wires or quantum dots. The first observation of this major change[2] had been predicted by a number of theoretical papers starting with the seminal work of Agranovitch *et al.*[3] Even before this paper, luminescence in quantum wells was unanimously attributed to free excitons, and the number of papers on the subject is so large that it is not possible to quote them in any reasonable way. Two questions however have aroused since the early papers on the subject: What is the influence of interface disorder on the properties of excitons? How do excitons form from unbound electron hole pairs?

The first question was initially raised by Weisbuch *et al.*,[4] again, and they proposed that the unavoidable interface roughness would give rise to an energy fluctuation of the confinement levels, translated into an inhomogeneous broadening of the exciton lines. Good samples were showing a linewidth corresponding to fluctuations by approximately one monolayer only. Further on, even better samples did show a splitting of the exciton lines corresponding to changes of the well width by exactly one monolayer.[5] More questions have been raised since then, in particular with the importance of disorder on the early secondary emission by quantum wells, attributed by Haacke *et al.* to Rayleigh scattering,[6] but the main picture has not really changed.

On the second question, how do excitons form? The debate has been attempted by several experimental and theoret-

ical groups. For instance, the quoted exciton formation times differ by orders of magnitude depending on the authors. A brief survey of the literature allows to find that experimentalists have reported formation times ranging from less than 10 ps up to about 1 ns (Refs. 7–12) and that theoretical values range from 100 ps (Refs. 13–16) to over 20 ns.[15] Clearly, the origin of this spreading in the reported values lies in the poor sensitivity of the experiments used in general to probe the exciton formation process, except for the case of the recent terahertz absorption experiments.[11]

A very interesting debate about the origin of the excitonic luminescence has been introduced by the group from Marburg.[18,19] The long formation time of excitons, together with the observation of PL at the exciton energy at the shortest times[7,8] led Kira, Koch *et al.*[18] to introduce the idea that a free electron hole plasma, properly including Coulomb correlation effects, should give rise to PL at the exciton energy, without the need for bound exciton pairs.

Quite recently two papers were published dealing with the exciton luminescence in QW showing very similar experimental results but with quite different interpretations. Our group has shown evidence for the fast exciton formation.[20,21] The groups from Marburg and Arizona[19] interpret their results using the model of *Coulomb correlated plasma* developed by Kira and Koch.[18] In the present work, we compare both approaches and draw conclusions about the validity of the two conflicting models. In addition, we give some insight into the exciton relaxation time. We will focus on two arguments: one is the fast exciton formation, already discussed in our previous letter[20] and second is the analysis of $1s$ and $2s$ excitonic transitions intensities.

We use a properly designed sample with a particularly high quality, together with a time-resolved photoluminescence set-up with improved sensitivity, to study the exciton formation and to give clues on the origin of luminescence in QW. The paper is organized as follows: in Sec. II we present our experimental results; in Sec. III we analyze the spectral
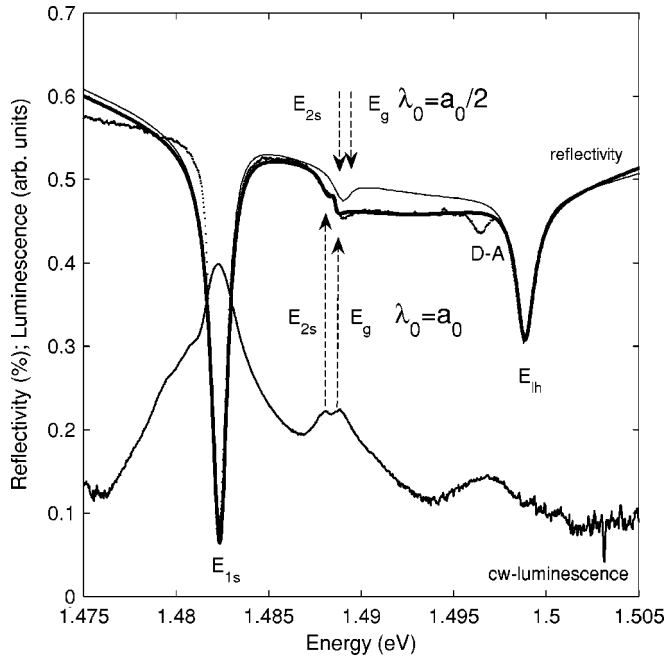
FIG. 1. Simulation of the sample reflectivity using transfer matrix method. Points, experimental data; thick line, calculations with $\lambda_0=a_0$; thin line, with $\lambda_0=a_0/2$. The corresponding energy transitions for E_{1s}, E_{2s}, E_g, E_{lh} are marked. *D-A* is the donor-acceptor transition in GaAs. The results of cw-luminescence are shown below for comparision.

origin of observed optical transitions; in Sec. IV we present two competitive approaches: in Sec. IV A we recall the results of the analysis based on the model of exciton formation proposed by Piermarocchi *et al.*[15,16] presented in our previous letter[20] and then in Sec. IV B we present some predictions of the model from Marburg.[18] Finally we compare both approaches with experimental data in Sec. IV C and draw out our conclusions in Sec. V.

II. EXPERIMENT

We have selected a particular sample, because of its high quality. The sample used for this study is a single $In_xGa_{1-x}As$ 80 Å quantum well (QW), with an indium content of about $x=5\%$ grown by molecular-beam epitaxy. This QW is embedded in the middle of a GaAs layer of total mean thickness λ (where λ corresponds to the wavelength of the excitonic resonance in the QW), which was grown over a 10 period distributed Bragg reflector (DBR). This DBR allows us to first measure the absorption of the sample in the reflection configuration without any preparation of the sample (Fig. 1). It also increases the optical coupling of the QW, but does not disturb appreciably the shape of the observed PL spectrum, because the resonance mode has a spectral width of about 40 nm, which is at least one order of magnitude larger than the width of any of the structures observed in luminescence. Such a DBR changes slightly the radiative properties of free carriers, but does not affect their relaxation properties which we are studying here. Through the specific growth process the thickness of all quantum structures changed along the

sample with a difference of about 4% over a distance of 25 mm. We chose certain position of the excitation in order to have an excitonic resonance in the middle of the λ layer resonance, as discussed in Ref. 21. The sample is kept in a helium bath cryostat and can be cooled down to 4.5 K. The position of the focal point of the optical excitation is controlled with precision of 1 μm. In the cw mode the sample is excited by a cw Ti:sapphire laser. For time-resolved luminescence spectroscopy we use spectrally filtered 100 fs pulses from the same Ti:sapphire laser working in the mode-locked regime. The interference spectral filter used as a pulse-shaper allows a spectral resolution of about 0.8–1.0 nm, and a temporal duration of about 1.2 ps. We used a 50 cm monochromator with a 600 lines per mm grating. The spectrum was recorded with a charge-coupled device (CCD) camera in cw and with a streak camera in the time-resolved experiment (resolution of 3 ps, photon-counting mode). The temporal resolution of the whole setup is limited to about 10–20 ps, due to the dispersion of the grating, allowing a 0.1 meV spectral resolution. The high quality of the sample is evidenced through optical measurements. We do not observe any Stokes shift between the absorption and PL at E_{1s}, E_{2s} and E_{plasma} (Fig. 1) as it was shown in our previous letter.[20]

All results presented here are collected with the excitation energy at $\hbar\omega=1.5174$ eV in the power range 1.0–300 μW (photon density $N_v=9\times10^8$–3×10^{11} photons/cm² per pulse; excitation spot diameter of 85 μm). We chose this wavelength for the following reasons: in order to characterize our sample, we continuously changed the excitation energy from 1.47 eV to over 1.62 eV using a Ti:sapphire tunable laser. We observe some changes in the spectrum, caused by the appearance of trion transition following the accumulation of electrons in the QW.[21] The characteristic features of our luminescence spectra (like enhanced intensity of excitonic luminescence or strong trion transition) are repeated every 43.5 meV, which suggest hot electron or hot exciton relaxation. The value 43.5 meV is close to the energy spacing ΔE for hot electron relaxation in GaAs [$\Delta E=\hbar\omega_{LO}\times(1+m_e/m_h)=41.4$ meV, $\hbar\omega_{LO}$ is the LO-phonon energy, m_e and m_h are the electron and hole effective masses in semiconductor[22]]. This energy scale shows that these features are not related to hot excitons relaxation via LO-phonon emission. We did not observe any resonance around 36 meV, that could only be linked with the direct process of exciton plus phonon creation. The direct process of creation of one exciton and one LO phonon is in all cases much weaker than electron-hole absorption. At first order it is even forbidden due to symmetry reasons, as it has been shown by Richard Planel.[23] The stronger probability involves at least two LO phonons, as it was shown by Clérot, Deveaud *et al.*[24] This process is only observed when very strong nonradiative recombination processes annihilate the free carrier contribution. Therefore by the selection of the excitation energy $\hbar\omega=1.5174$ eV we get rid of the carrier accumulation in our QW and we exclude the resonant LO phonon creation of excitons.

III. DETERMINATION OF EXCITON BINDING ENERGY

Proper identification of the structures observed in our absorption and photoluminescence experiments is very crucial

for our reasoning.[20,21] Our recognition differs from the identification proposed by Chatterjee *et al.*[19] The main difference lies in the attribution of the heavy-hole excited state 2*s* and plasma transition to the measured spectrum (Fig. 1). The peak in the luminescence around 1.4888 eV in Fig. 1 originates from the plasma transition and not from the 2*s* excited heavy-hole exciton state. This excited 2*s* peak is clearly seen at 1.4882 eV at low temperatures in cw-experiments[21] (Fig. 1) and when the temperature of carriers is larger (above 15 K) the ionization process is efficient enough to dissociate this state.

The next confirmation of our identification comes from the calculation of the reflectivity spectrum of our sample. We use a transfer-matrix approach in which we included the structure of our sample, i.e., the thickness of the λ layer, QW in the middle, and 10 periods of DBR. The thickness of subsequent layers were taken from the technological data. Due to the wedge we had to introduce a multiplicative factor (the same for all layers) to include the change in the thickness across our sample.

To calculate the oscillator strengths 1*s*, 2*s* and continuum states we applied the model of Atanasov *et al.*[25,31] In this approach, the exciton Bohr radius in $In_xGa_{1-x}As$ quantum well λ_0 is calculated by means of variational method and is different from the three dimensional Bohr radius a_0. We did not calculate λ_0. Since we use a sample of 8.0 nm $In_xGa_{1-x}As$ quantum well with relatively low In content $x \approx 5\%$, we set $\lambda_0 = a_0$. In an ideal two-dimensional case λ_0 should be equal to $a_0/2$.

We corrected some obvious errors in the formulas in the paper of Atanasov *et al.*,[25] and we use the following equations for the excitonic $\alpha_X(\omega)$ and free carrier $\alpha_{fc}(\omega)$ absorption,[32]

$$\alpha_X(\omega) = \frac{8C_0}{\lambda_0^2}\left[\frac{1}{\pi}\sum_{n=1,2}\frac{4(\hbar\omega)\Gamma_{X,n}E_n(2n-1)^{-3}}{(E_n^2-(\hbar\omega)^2)^2+4(\hbar\omega)^2\Gamma_{X,n}^2}\right],$$

(1a)

$$\alpha_{fc}(\omega) = \frac{C_0}{a_0^2}\left[\frac{1}{\pi}\int\frac{4(\hbar\omega)\Gamma_{fc}E'S_{2D}(E_k/R_y)}{(E'^2-(\hbar\omega)^2)^2+4(\hbar\omega)^2\Gamma_{fc}^2}dE_k\right]$$

(1b)

$(E' = E_g + E_k)$ where E_g is the gap energy, $E_k = \hbar^2 k^2/2m_r$ is the kinetic energy of free carriers with momentum k, m_r is the reduced mass of electron and hole, $\Gamma_{X,n}$ and Γ_{fc} are the broadening of the exciton and free carrier transitions, respectively, $n = 1s, 2s$ indicates excitonic states, R_y is the exciton Rydberg energy, the parameter C_0 is

$$C_0 = \frac{e^2|\hat{e}\mathbf{p}_{cv}|^2}{2n_r c\varepsilon_0 m_0^2\omega(L_w+L_B)}.$$

e is the electron charge, $|\hat{e}\mathbf{p}_{cv}|$ is the dipole matrix element, the refractive index $n_r = \sqrt{\varepsilon_B}$, where $\varepsilon_B(\varepsilon_{QW})$ is the dielectric constant of the barrier (quantum well) semiconductor, ε_0 is the vacuum dielectric constant, c is the light velocity, m_0 is the free electron mass, L_w and L_B are the length of a quantum well and a barrier, respectively. The three-dimensional exciton Bohr radius a_0, the exciton Rydberg energy R_y, and the

Sommerfeld enhancement factor in two dimensions S_{2D} are, respectively,

$$a_0 = \frac{\hbar^2}{m_r}\left(\frac{4\pi\varepsilon_0\varepsilon_{QW}}{e^2}\right), \quad R_y = \frac{m_r e^4}{2\hbar^2(4\pi\varepsilon_0\varepsilon_{QW})^2},$$

$$S_{2D}(\varepsilon) = \frac{2}{1+\exp(-2\pi/\sqrt{\varepsilon})}.$$

The final results of our calculations are shown in Fig. 1 by a thick line. As a fitting parameter we use C_0/a_0 (oscillator strength of 1*s* light hole exciton was taken three times smaller than heavy-hole one), the following values of the broadening: $\Gamma_{X,1s} = 0.38$ meV, $\Gamma_{X,2s,3s} = 0.50$ meV and $\Gamma_{fc} = 0.08$ meV and the energies of the transition: $E_{1s} = 1.48242$ eV, $E_{2s} = 1.48822$ eV, $E_{3s} = 1.48840$ eV, $E_{1s,lh} = 1.49880$ eV, $E_g = 1.48860$ eV. One can notice a very good agreement between the transfer matrix method and experiment. The small deviation at lower energies is probably caused by the use of a constant value for GaAs, $In_xGa_{1-x}As$, and AlAs refractive indexes. The result for the ideal two-dimensional case $\lambda_0 = a_0/2$ is also shown in Fig. 1 (thin line). However it is impossible to fit our experimental data with the perfect 2D exciton. Even a change of the computed energy of 2*s* transition to 1.4888 eV does not yield a good fit. This is an important remark in which our interpretation of the experimental data differs from the paper of Chatterjee *et al.*[19] and we will discuss it further in Sec. IV B. It is worth mentioning that also the exciton binding energy in our QW has a smaller value and is more reasonable than one predicted from paper of Chatterjee *et al.*[19]

IV. DISCUSSION

In the next two paragraphs we are going to present both competitive approaches and compare them with our experimental results.

A. Model of the formation of excitons

The analysis of our experimental data allowed us to draw some conclusions about the formation of excitons. This problem was developed in details in our previous letter[20] therefore in this chapter we will briefly summarize our results and give some more insight about the fitting procedure.

Our large dynamical range allows us to measure the free carrier temperature directly from the spectrum for all delays longer than 100 ps.[20] The PL of free carriers above the band edge provides a direct measure of the relative variations of the population of free electrons and holes and in QWs follows the relation:

$$n \propto \sqrt{I_{PL}^{fc}T},$$

(2)

where I_{PL}^{fc} is the intensity of free carriers luminescence and T is the temperature.[20]

Knowing the temporal evolution of the concentration of free carriers in QW deduced from Eq. (2) one can relate it with the exciton dynamic. Indeed, we get two rate equations for the population of free carriers n and of excitons X,

$$\frac{dn}{dt} = -\gamma C n^2 + \gamma CKX - \frac{n}{\tau_{nr}} - Bn^2, \tag{3a}$$

$$\frac{dX}{dt} = \gamma C n^2 - \gamma CKX - \frac{X}{\tau_D}. \tag{3b}$$

The temporal evolution of the free carrier concentration [Eq. (3a)] is governed by the electron-hole bimolecular recombination rate B, the nonradiative carrier decay time τ_{nr}, and the formation and ionization of excitons. In our calculations we use the approach proposed by Piermarocchi *et al.*[16] in which population of excitons is built up due to the bimolecular formation. This bimolecular formation rate C depends upon both carrier and lattice temperature through the interaction with optical and acoustic phonons. We introduced a multiplication factor γ by which the measured formation rate in our InGaAs QW is changed compared to the theoretical value obtained for GaAs. Our rate equations complete the microscopic theory of carrier and exciton dynamic in QW proposed by Piermarocchi *et al.*[15,16] and $K(T)$ is an equilibrium coefficient given by mass action law (Saha equation) for excitons.

In our previous rate equations[20] the term CN_{eq}^2 determined by Saha equation was used. This term corresponded to equilibrium carrier and exciton concentrations. Instead of it, now we use in Eq. (3) the total exciton concentration CKX. This approximation gives the same limit in case of equilibrium conditions but is more general and more realistic for low exciton concentrations. With the term CKX we got practically the same results as in our previous paper.[20]

B. Model of the Coulomb correlated plasma

The above model, using simple rate equations, may seem too simplistic. However it contains all components of what should be a full model, and the values of C introduced in our approach have been taken from a full computation,[15,16] as it was already mentioned before. There exists an alternative approach proposed by Kira, Koch *et al.*[18] According to this theoretical description excitonic transition observed in nonresonant PL experiments does not necessarily originate from a macroscopic population of excitons. This excitonic like transition could be due to free carrier luminescence, without the need for bound pairs. In the following paragraph we will shortly present this model for those who are not very familiar with it, before comparing the model with our experimental results.

In this density-matrix many-body theory, the dynamic Hartree-Fock approximation leads to the luminescence consisting in two source terms: excitonic and free carriers.[28] The quantum well luminescence intensity is finally expressed using Elliott-type formula,[15,16]

$$I_{PL} = -\frac{2}{\hbar} \mathrm{Im}\left[|\mathcal{F}_q|^2 \sum_\nu |\phi_{\nu,q}^r(0)|^2 \frac{\langle X_{\nu,q}^\dagger X_{\nu,q}\rangle_S + \Delta\langle X_{\nu,q}^\dagger X_{\nu,q}\rangle}{\hbar\omega_q - E_G - E_{\nu,q} + i\gamma_\nu} \right]. \tag{4}$$

$X_\nu^\dagger(X_\nu)$ means the creation (annihilation) operator of excitons with the quantum number ν; ω is the photon wavelength; E_G

is the energy gap in the semiconductor quantum structure; E_ν is the energy corresponding to state ν, given by the solution of the generalized Wannier equation, and γ_ν is the broadening.

The term $\Delta\langle X_\nu^\dagger X_\nu\rangle$ corresponds to all off-diagonal transition correlations attributed to the number of excitons.[17] Therefore this is the source term for the excitonic luminescence. The other important term in this approach is the singlet Hartree-Fock term

$$\langle X_\nu^\dagger X_\nu\rangle_S = \sum_k |\phi_\nu^r(k)|^2 f_k^e f_k^h, \tag{5}$$

where f_k^e and f_k^h denotes electron and hole distributions, $\phi_\nu^r(k)$ is the right-hand generalized Wannier exciton wave function. This term originates from Coulomb correlated electron-hole plasma. Thus the conclusion from the presented theoretical approach is that, even with vanishing exciton correlations $\Delta\langle X_\nu^\dagger X_\nu\rangle$, the pure plasma singlet term Eq. (5) results in a strong peak at all exciton resonances ($1s$, $2s$, etc.) and therefore the standard photoluminescence experiment cannot distinguish between contributions from exciton correlations and Coulomb correlated plasma. The origin of the possible emission of light in the excitonic energy by unbound pairs lies in the Coulomb mediated collisions allowing the remaining pairs to carry away the excess energy.

The interest of such a closed format equation is that it allows experimentalist to get an approximate line shape without heavy computations. We would like to discuss the extreme case—the QW luminescence of the Coulomb correlated plasma without any excitons. We neglect the term $\Delta\langle X_\nu^\dagger X_\nu\rangle$ and we calculate only Eq. (5). We found that the temperature dependence of $1s$ and $2s$ plasma transitions is different from that of the temperature dependence of $1s$ and $2s$ exciton transitions.

In a low density regime the generalized Wannier exciton wave function $\phi_\nu^r(k)$ might be simplified by the simplest exciton Wannier function $\psi_\nu(k)$. Let us consider the two-dimensional (2D) excitonic wave functions $1s$ and $2s$,[29]

$$\psi_{1s}(r) = \sqrt{\frac{8}{\pi a_0^2}} e^{-2r/a_0}, \tag{6a}$$

$$\psi_{2s}(r) = \sqrt{\frac{8}{27\pi a_0^2}}\left(1 - \frac{4}{3a_0}\right) e^{-2r/3a_0}, \tag{6b}$$

where a_0 is the three-dimensional (3D) Bohr radius of the exciton introduced before. From Eq. (6) one can calculate the Fourier-transform functions $\psi_{1s}(k)$ and $\psi_{2s}(k)$:

$$\psi_{1s}(k) = \sqrt{\frac{8}{\pi a_0^2}} \frac{2a_0^2}{(4 + a_0^2 k^2)^{3/2}}, \tag{7a}$$

$$\psi_{2s}(k) = \sqrt{\frac{8}{27\pi a_0^2}} \frac{54a_0^2(-4 + 9a_0^2 k^2)}{(4 + 9a_0^2 k^2)^{5/2}}. \tag{7b}$$

The Maxwell-Boltzmann distribution of electrons f_e and holes f_h is given by

$$f_\nu(k) = e^{-\beta\mu_\nu}e^{-\beta\hbar^2k^2/2m_\nu}, \tag{8}$$

where $\nu=e$, h and $\beta=1/k_BT$. The chemical potentials μ_e and μ_h might be calculated from the total concentration of the carriers n

$$\mu_\nu = -k_BT\ln\left(\frac{2\pi\hbar^2 n}{m_\nu k_BT}\right). \tag{9}$$

Thus the Coulomb correlated plasma Hartree-Fock term is given by the integral

$$\langle X_\nu^\dagger X_\nu\rangle_S = 2\pi e^{-\beta\mu_\nu}\int_0^\infty ke^{-bk^2}|\psi_\nu(k)|^2 dk, \tag{10}$$

where $b=b(T)=\hbar^2/2m_r k_BT$ and m_r is the reduced exciton mass. Then the results of the integration of Eq. (10) for $1s$ and $2s$ transitions are as follows:

$$\langle X_{1s}^\dagger X_{1s}\rangle_S = \frac{\hbar^2 n}{m_r k_BT}[1 - s + se^sE_1(s)], \tag{11a}$$

where $s=4b/a^2$, and

$$\langle X_{2s}^\dagger X_{2s}\rangle_S = \frac{\hbar^2 n}{m_r k_BT}[1 - s - 3s^2 - s^3 + (3 + 4s + s^2)s^2 e^s E_1(s)], \tag{11b}$$

where $s=4b/9a^2$. The function $E_1(s)$ means the exponential integral.

Having Eq. (4) and Eqs. (11a) and (11b) one can calculate the luminescence of the Coulomb correlated plasma

$$I_{\text{PL}}^\nu \propto \frac{\gamma_\nu|\psi_\nu(0)|^2\langle X_\nu^\dagger X_\nu\rangle_S}{(\hbar\omega - E_{\text{G}} - E_\nu)^2 + \gamma_\nu^2}, \tag{12}$$

where $\nu=1s$, $2s$ and the oscillator strength $|\psi_\nu(0)|^2=8/a^2$ for $1s$ and $8/27a^2$ for $2s$.

The results are shown in Fig. 2 for GaAs parameters and arbitrary chosen energy transitions E_{1s} and E_{2s}; $\gamma=1.0$ meV. In our model calculations we neglected the continuum states, so this plot is not valid for the energies above E_g (about 1.492 eV). One can notice that the temperature dependence of the $1s$ and $2s$ luminescence is counterintuitive, because one expects that for the lowest temperatures the $1s$ line dominates over the spectrum. According to our calculation, at 1.0 K the $2s$ transition is almost as equally intense as $1s$.

The reason for this is explained in Fig. 3. We plot the relevant integrals $k|\psi_\nu(k)|^2$ together with the Boltzmann occupation $\exp(-bk^2)$ at a relevant (small) temperature. Obviously, the $2s$ state is much more concentrated at small momentum than $1s$. This reflects the larger extension of $2s$ in real space [the relevant radius is $a_n=(n-1/2)a_0$ for strict 2D with a_0 being the 3D exciton Bohr radius]. Now, the reasoning goes as follows: at large temperatures, the occupations are nearly the same due to the proper normalization of the wave function in momentum space. However, at low temperatures, the Boltzmann factor gives much more weight to small k, which enhances the $2s$ occupation. The ratio N_{2s}/N_{1s} is directly given by $|\psi_{2s}(k=0)/\psi_{1s}(k=0)|^2=27$. It equals the (inverse) oscillator strength ratio $|\psi_{1s}(r=0)/\psi_{2s}(r=0)|^2$ (an
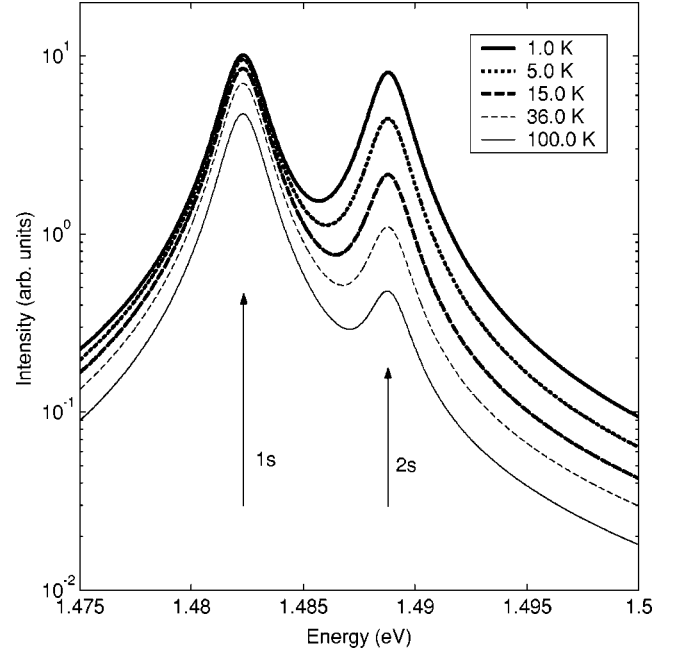

FIG. 2. The Coulomb correlated plasma luminescence calculated according to Eq. (12) for different temperatures. The energetic positions of $1s$ and $2s$ transitions are chosen arbitrary to remind our experimental results. The results for the energy greater than E_g (about 1.492 eV) are not valid, since the continuum states are not included in the calculation.

accidental coincidence), and therefore the low-temperature limit approaches unity in Fig. 4.

Similarly, Eqs. (11a) and (11b) increase monotonically with temperature and finally saturate. The $2s$ function saturates faster than the $1s$, which has an influence on the relative
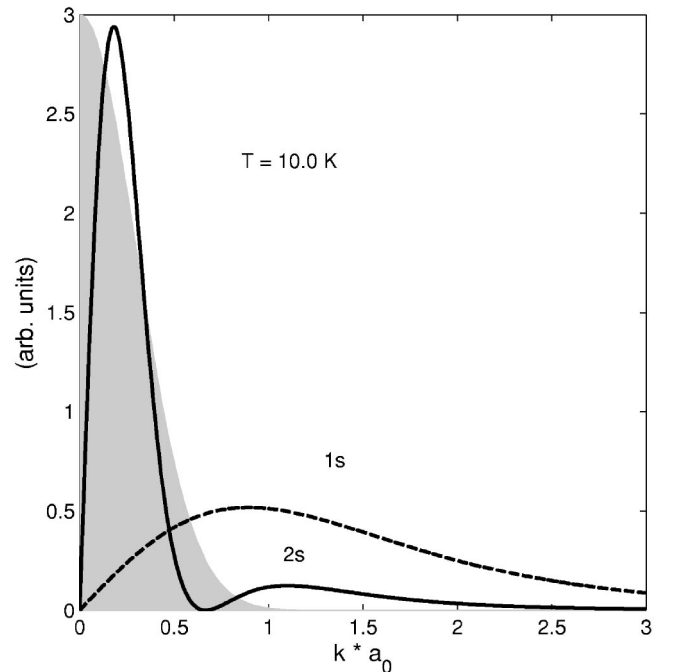

FIG. 3. The relevant integrals $k|\psi_\nu(k)|^2$ for $1s$ and $2s$ states together with the Boltzmann occupation at 10.0 K (shadowed).

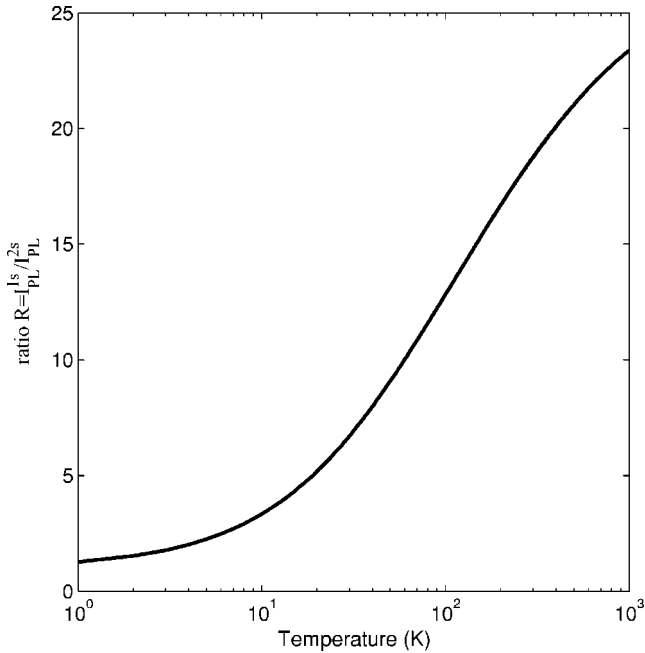FIG. 4. Temperature dependence of the ratio of the maxima $R = I_{PL}^{1s}/I_{PL}^{2s}$ calculated with the results of Eq. (12).

temperature dependence. For very high temperatures the intensity ratio reflects the difference in the oscillator strength. The temperature dependence of the ratio $R = I_{PL}^{1s}/I_{PL}^{2s}$ transitions is shown in Fig. 4.

In order to be able to perform these calculations, we simplified the problem by using a simple Wannier exciton wave function $\psi_\nu(k)$ instead of a right-hand generalized Wannier exciton wave function $\phi_\nu^r(k)$ (which is fully justified in a low density regime). However the observation shown in Fig. 3 is very similar also for $\phi_\nu^r(k)$ and therefore our arguments are also valid in this case. The general tendency of R shown in Fig. 4 is that R increases with the temperature. The full calculations which take into account also the carrier density influence on the wave function $\phi_\nu^r(k)$ and on the line broadening γ_ν give very similar results which differ only by the factor of 2 for the densities of $10^8 - 10^9$ cm^2. With this factor of 2, R does not depend on density, but only on temperature.

C. Comparison with experiment

1. Model of the formation of excitons

Increasing the carrier density leads to a faster formation of excitons, because it gives rise to an increased probability of binding one electron and one hole through interaction with phonons. This important theoretical prediction is indeed confirmed in our experiment. The formation time $\tau_f := (\gamma C n)^{-1}$, measured over two orders of magnitude in density 100 ps after the initial excitation, changes from less than 10 ps for the highest density to 570 ps for the lowest one. This τ_f evolves as the plasma concentration and temperature change and, 1 ns after the excitation, binding of free carriers into excitons is as long as 130 ps to 1100 ps, respectively. Thus the spread of the experimental values of τ_f found in the

literature[7,9–11] might simply be related to different experimental conditions.

From the comparison of the calculated and measured luminescence intensity presented in our letter in Fig. 4,[20] one can estimate two important parameters used in Eq. (3): τ_D and B. Indeed, the value of τ_D depends on the theoretical approach. One of the possible calculations of τ_D is given by Piermarocchi.[15] To be consistent with his theory we might use his calculation presented in Fig. 5 therein. However the simplest approximation of his results introduces other parameters like "offset" and "slope" of the carriers' temperature dependence. From Eq. (2) there is only one accessible quantity: the density of carriers n and one gets very similar fit of n for the parameters as different as: $\tau_D = 30 \times T$, $\tau_D = 300 + 3 \times T$, $\tau_D = 300 + 20 \times T$, $\tau_D = 700$, etc. (τ_D is in ps, temperature T is in K). Therefore it is quite difficult to judge which dependence is correct. However from the fit to the excitonic luminescence presented in our letter[20] one can estimate the value of τ_D more precisely. The thermalized exciton decay time τ_D is not necessarily the same for all densities and is not necessarily constant (it should depend on temperature). We decided arbitrarily not to play with too many fitting parameters and we believe that one value of τ_D explains sufficiently well our results. In fact, for the lowest densities the decay of the excitonic luminescence is limited by the long exciton formation time and not the exciton thermalization! One can also estimate the value of B. In our case we use 15 K value given by Matsusue [$B = 10^{-3}$ cm^2/s (Ref. 26)] shortened by a factor 10 due to the DBR, so our $B(T) = 0.01 \times (15/T)$ cm^2/s, temperature T is in K. This rate is roughly two orders of magnitude smaller than τ_D for the free carriers in the density range considered.

It is worth mentioning that this enhancement of the exciton radiative decay time does not influence strongly τ_D, which is the thermalized decay time for the whole population of excitons, i.e., dark and radiative ones. τ_D depends mostly on the different processes of the exciton relaxation to the radiative cone, which are not influenced by our weak cavity. Therefore our analysis gives the order of magnitude of the exciton recombination in QW for given temperatures and densities. The value of $\tau_D = 700$ ps is not far from the theoretical prediction given by Andreani *et al.*,[27] who found that in 100 Å GaAs/Al$_{1-x}$Ga$_x$As QW the radiative decay changes with the temperature with a slope of about 34 ps/K. We do not know the temperature of excitons, we even do not know whether their distribution is thermal or not, however assuming that the exciton temperature is around 20 K (i.e., it is not too far from the carrier temperature) one can find radiative lifetime τ_D just around 700 ps. The important point is that we use the temperature of the excitons, not of the lattice.

We think that the conflicting model of the *Coulomb correlated plasma* of the group of Marburg[18] cannot describe this initial carriers concentration drop since the exciton formation time that they compute is much longer in their approach.

2. Model of the Coulomb correlated plasma

In order to compare the above theoretical predictions of $R = I_{PL}^{1s}/I_{PL}^{2s}$ with our experimental results we tried to estimate

the temperature dependence of the experimental intensities $I_{PL,exp}^{1s}(T)$ and $I_{PL,exp}^{2s}(T)$. For each time after the initial excitation we know the temperature of the carriers.[20] Therefore we could deduce the relationship between the intensity and the temperature. For each time the intensity $I_{PL,exp}^{1s}(T)$ was taken as an integral of our spectrum over the energies 1.478–1.486 eV. The similar integral 1.487–1.495 eV was taken for the total $2s$ $[I_{PL,exp}^{2s}(T)]$ and free carrier transitions $[I_{PL,exp}^{fc}(T)]$. Unfortunately, our analysis of R might be influenced by two major problems. The first one is related to the separation of the $I_{PL,exp}^{2s}$ and $I_{PL,exp}^{fc}$ transitions (since only $I_{PL,exp}^{2s}+I_{PL,exp}^{fc}$ can be accessed) and the second is related to the difference in the temperature of excitons and carriers.

One of the possible ways to solve the first problem is to use both the known experimental ratio R_{exp}:

$$R_{exp} = \frac{I_{PL,exp}^{1s}(T)}{I_{PL,exp}^{2s}(T) + I_{PL,exp}^{fc}(T)}$$

and the theoretical calculation of $I_{PL}^{fc}(T)$ is given by bimolecular recombination $I_{PL}^{fc}(T) = Bnp$. The validity of the latter has already been discussed in Sec. IV A for *excitons plus free carriers* and *Coulomb correlated plasma*[18] models. Thus we assume that the intensity $I_{PL,exp}^{fc}(T)$ is proportional to n^2/T with a certain coefficient $c > 0$ (theoretically $c = BT$). We finally get for $I_{PL}^{1s}(T)$ and $I_{PL}^{2s}(T)$:

$$I_{PL}^{1s}(T) \approx I_{PL,exp}^{1s}(T), \tag{13a}$$

$$I_{PL}^{2s}(T) \approx \frac{1}{R_{exp}} \left(I_{PL,exp}^{1s}(T) - cR_{exp}\frac{n^2}{T} \right), \tag{13b}$$

where n might be calculated from Eq. (3) and the requirement $I_{PL}^{2s}(T) \geq 0$ gives the upper limit for c. Even if one disagrees with our calculations of n and assumes that the transition observed in 1.4888 eV comes mostly from the $2s$ transition (as it is done by Chatterjee *et al.*[19]) one can set $c = 0$ or very close to zero. The ratio R is then calculated from Eq. (13).

The other open question is about the exciton and free-carrier temperatures. From the experimental results we only determined the plasma temperature. In the *Coulomb correlated plasma* approach all optical transitions originate from the plasma, therefore the temperature in the whole system is the same. In the case of the *excitonic population* the relative excitons-plasma temperature might be different, because excitons formed by the phonon emission have higher temperature. Thus one can assume an exciton temperature of the form of $T + T_{eff}$, where T denotes a free carrier temperature and $T_{eff} \geq 0$ is the difference between the exciton and free-carriers temperature. Moreover T_{eff} depends on the carriers and excitons concentration, because the exciton-carrier interaction is more efficient at high densities and therefore T_{eff} should decrease with density. The exact description requires theoretical models and yet more assumptions.

Since the parameters c and T_{eff} might be chosen arbitrarily we do not want to discuss their exact value. What we wanted to show is the general experimental tendency, which can be compared with the results of the model of the *population of*
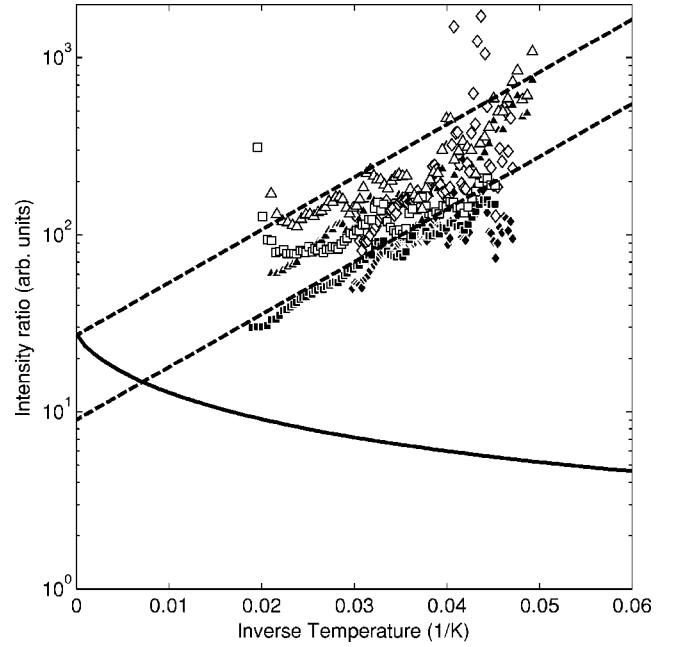

FIG. 5. Intensity ratio $R = I_{PL}^{1s}/I_{PL}^{2s}$ as a function of the inverse temperature. The points represent experimental results. Black points are with $c = 0$, white points are with an arbitrary small c. Errors are not shown. The dashed lines correspond to the Boltzmann factor $\exp[(E_{1s} - E_{2s})/k_B T]$ with the oscillator strength ratio 27 (upper one) and 9 (lower one). The solid line is the ratio presented in Fig. 4 shown for comparison. The effective temperatures $T_{eff} = 15$ K were taken for the lowest (diamonds), $T_{eff} = 10$ K for middle (squares), and $T_{eff} = 5$ K for highest (triangles) carrier density.

excitons and the *Coulomb correlated plasma* approach.

In Fig. 5 we present the results of the above analysis. The solid line is the ratio R presented in Fig. 4 plotted in the inverse temperature. This line represents nonthermal $1s$ and $2s$ intensity ratio derived from the *Coulomb correlated plasma* approach. The two dashed lines in this figure come from the simplest model of the thermal Boltzmann distribution of the populations of $1s$ and $2s$ excitons $\exp[(E_{1s} - E_{2s})/k_B T]$, calculated with ideal 2D and 3D oscillator strengths ratio (3^3 and 3^2, respectively). The energetic difference $E_{1s} - E_{2s}$ was taken from the fit in Fig. 1. The points represent experimental data—we calculated the $R = I_{PL}^{1s}/I_{PL}^{2s}$ according to Eq. (13) as a function of exciton temperature for three different excitation densities. The effective temperatures $T_{eff} = 15$ K were taken for the lowest (diamonds), $T_{eff} = 10$ K for middle (squares), and $T_{eff} = 5$ K for highest (triangles) carrier density. These effective temperatures were chosen arbitrarily, in order to superimpose experimental points between both dashed lines. The experimental points with $c = 0$ are marked in black. This value of c corresponds to the limit when $I_{PL}^{2s} \approx I_{PL,exp}^{2s} + I_{PL,exp}^{fc}$. The open points are plotted with an arbitrary small c, which always increases R. One can see, that for any parameters T_{eff} and c it is impossible to get the nonthermal temperature dependence calculated with the model of the *Coulomb correlated plasma* and Eq. (12). What is important is not the actual value of the fitting parameters but the fact, that in the case of the model of *excitons and free carriers* it is possible to find some reasonable pa-

rameters which give qualitative agreement to some simple theoretical predictions (like the thermal Boltzmann distribution).

Therefore we think that our experimental data gives strong support for all the theoretical models which take into account the existence of the population of excitons in excited quantum wells. In the paper of Chatterjee *et al.*[19] the authors admit that one has to add the arbitrary population of excitons to explain the luminescence spectrum of quantum wells. This statement was not clear at all in the previous papers.[18] Our experiments even evidence that the dominant feature of the luminescence of QW comes from the population of excitons while the contribution of Coulomb correlated plasma may be neglected within discussed temperature and density ranges.

V. SUMMARY

Our experimental data and analysis give strong support for all the theoretical models which take into account the formation of the *population of excitons* in excited quantum wells. This conclusion is based on two major arguments: one is the fast exciton formation and second is the analysis of relative 1*s* and 2*s* excitonic transitions intensities.

We have described the results of the time-resolved photoluminescence study of a very high quality InGaAs QW sample where the contributions at the energy of the exciton and at the band edge can be clearly separated. We demonstrated that a simple rate equation together with the exciton formation theory of Piermarocchi *et al.*[16] can describe the experimental data of the evolution of carriers concentration. Especially we demonstrated the fast exciton formation at high densities. By the estimation of the time dependence of the excitonic and free carriers luminescence we show that the exciton luminescence dominates the spectrum at all times for all realistic pumping intensities used in time-resolved experiments.[20]

We drew out some conclusions about the relative luminescence intensities of 1*s* and 2*s* transitions in QW and we show that these transitions might be modeled by a simple thermal occupation of both excitonic states. This is in clear contradiction with the *Coulomb correlated plasma* model which predicts nonthermal behavior.

*Permanent address: Institute of Experimental Physics, Warsaw University, Hoża 69, 00-681 Warsaw, Poland.

[1] C. Weisbuch, R. C. Miller, R. Dingle, A. C. Gossard, and W. Wiegmann, Solid State Commun. **37**, 219 (1981).

[2] B. Deveaud, F. Clérot, N. Roy, K. Satzke, B. Sermage, and D. S. Katzer, Phys. Rev. Lett. **67**, 2355 (1991).

[3] V. M. Agranovitch and O. A. Dubovskii, JETP Lett. **3**, 223 (1966).

[4] C. Weisbuch, R. Dingle, A. C. Gossard, and W. Wiegmann, Solid State Commun. **38**, 709 (1981).

[5] B. Deveaud, J. Y. Emery, A. Chomette, B. Lambert, and M. Baudet, Appl. Phys. Lett. **45**, 1078 (1984).

[6] S. Haacke, R. A. Taylor, R. Zimmermann, I. Bar-Joseph, and B. Deveaud, Phys. Rev. Lett. **78**, 2228 (1997).

[7] T. C. Damen, J. Shah, D. Y. Oberli, D. S. Chemla, J. E. Cunningham, and J. M. Kuo, Phys. Rev. B **42**, 7434 (1990).

[8] G. R. Hayes and B. Deveaud, Phys. Status Solidi A **190**, 637 (2002).

[9] D. Robart, X. Marie, B. Baylac, T. Amand, M. Brousseau, G. Bacquet, G. Debart, R. Planel, and J. M. Gérard, Solid State Commun. **95**, 287 (1995).

[10] B. Deveaud, B. Sermage, and D. S. Katzer, J. Phys. IV **3**, 11 (1993).

[11] R. A. Kaindl, M. A. Carnahan, D. Hgele, R. Lvenich, and D. S. Chemla, Nature (London) **423**, 734 (2003).

[12] H. W. Yoon, D. R. Wake, and J. P. Wolfe, Phys. Rev. B **54**, 2763 (1996).

[13] B. K. Ridley, Phys. Rev. B **41**, 12 190 (1990).

[14] A. Thilagam and Jai Singh, J. Lumin. **55**, 11 (1993).

[15] C. Piermarocchi, F. Tassone, V. Savona, A. Quattropani, and P. Schwendimann, Phys. Rev. B **53**, 15 834 (1996); C. Piermarocchi, V. Savona, A. Quattropani, P. Schwendimann, and F. Tassone, Phys. Status Solidi A **164**, 221 (1997).

[16] C. Piermarocchi, F. Tassone, V. Savona, A. Quattropani, and P. Schwendimann, Phys. Rev. B **55**, 1333 (1997).

[17] W. Hoyer, M. Kira, and S. W. Koch, Phys. Rev. B **67**, 155113 (2003).

[18] M. Kira, F. Jahnke, and S. W. Koch, Phys. Rev. Lett. **82**, 3544 (1999); **81**, 3263 (1998); M. Kira, F. Jahnke, W. Hoyer, and S. W. Koch, Prog. Quantum Electron. **23**, 189 (1999).

[19] S. Chatterjee, C. Ell, S. Mosor, G. Khitrova, H. M. Gibbs, W. Hoyer, M. Kira, S. W. Koch, J. P. Prineas, and H. Stolz, Phys. Rev. Lett. **92**, 067402 (2004).

[20] J. Szczytko, L. Kappei, J. Berney, F. Morier-Genoud, M. T. Portella-Oberli, and B. Deveaud, Phys. Rev. Lett. **93**, 137401 (2004).

[21] J. Szczytko, L. Kappei, F. Morier-Genoud, T. Guillet, M. T. Portella-Oberli, and B. Deveaud, Phys. Status Solidi C **1**, 493 (2004).

[22] S. Permogorov, Phys. Status Solidi B **68**, 23 (1975).

[23] Richard Planel, Ph.D. thesis, Laboratoire de Physique de l'Ecole Normale Supériere, Paris VII, 1977.

[24] F. Clérot, B. Deveaud, A. Chomette, A. Regreny, and B. Sermage, Phys. Rev. B **41**, 5756 (1990).

[25] R. Atanasov, F. Bassani, A. D'Andrea, and N. Tomassini, Phys. Rev. B **50**, 14381 (1994).

[26] T. Matsusue and H. Sakaki, Appl. Phys. Lett. **50**, 1429 (1987).

[27] L. C. Andreani, F. Tassone, and F. Bassani, Solid State Commun. **77**, 641 (1991).

[28] S. W. Koch, T. Meier, W. Hoyer, and M. Kira, Physica E

(Amsterdam) **14**, 45 (2002).

[29] H. Haug and S. Koch, *Quantum Theory of the Optical and Electronic Properties of Semiconductors* (World Scientific, Singapore, 1990).

[30] R. Atanasov, F. Bassani, and V. M. Agranovich, Phys. Rev. B **49**, 2658 (1994).

[31] In the paper of R. Atanasov *et al.* (Ref. 25) the formulas (33) and (34) therein should be corrected. In the part of $\Gamma_X 27^{1-n}/E_n$ and $\Gamma_{fc} S_{2D}(\varepsilon)/E_n$ there should be rather multiplication than division, so it must be $\Gamma_X 27^{1-n} \times E_n$ and $\Gamma_{fc} S_{2D}(\varepsilon) \times E_n$, which would be consistent with Ref. 30 [and Eqs. (9) and (10) in Ref. 30]. Also in Eq. (33) there should be no $\hbar\omega$ in the coefficient before the integral [again see Eqs. (9) and (10) in Ref. 26: $E^2=(\hbar\omega)^2$ is in the denominator and absorption coefficient $\alpha(\omega)=(4\pi)\omega/n_r c \times \mathrm{Im}(\chi(\omega))$].

[32] In fact for the calculations of transfer matrix we use optical susceptibility, however the relationship between absorption and optical susceptibility is straightforward.